applied sciences

MDPI

Review

Physical, Chemical, and Genetic Techniques for Diatom Frustule Modification: Applications in Nanotechnology

Alessandra Rogato [1,2] and Edoardo De Tommasi [3,*]

1 Institute of Biosciences and Bioresources, National Research Council, Via P. Castellino 111, 80131 Naples, Italy; alessandra.rogato@ibbr.cnr.it
2 Department of Integrative Marine Ecology, Stazione Zoologica Anton Dohrn, 80121 Naples, Italy;
3 Institute of Applied Sciences and Intelligent Systems, National Research Council, Via P. Castellino 111, 80131 Naples, Italy
* Correspondence: edoardo.detommasi@na.isasi.cnr.it

Received: 29 September 2020; Accepted: 3 December 2020; Published: 6 December 2020

Abstract: Diatom frustules represent one of the most complex examples of micro- and nano-structured materials found in nature, being the result of a biomineralization process refined through tens of milions of years of evolution. They are constituted by an intricate, ordered porous silica matrix which recently found several applications in optoelectronics, sensing, solar light harvesting, filtering, and drug delivery, to name a few. The possibility to modify the composition and the structure of frustules can further broaden the range of potential applications, adding new functions and active features to the material. In the present work the most remarkable physical and chemical techniques aimed at frustule modification are reviewed, also examining the most recent genetic techniques developed for its controlled morphological mutation.

Keywords: diatoms; biomaterials; biomineralization; hybrid nanomaterials; surface functionalization; nanotechnologies; sensing; genetic engineering

1. Introduction

Many living organisms, from unicellular to multicellular ones (e.g., bacteria, protists, plants, invertebrates and vertebrates), are able to produce minerals to develop peculiar features such as shells, bones, teeth or exoskeleton. This process, defined as biomineralization, involve over 62 different biominerals (mainly calcium carbonates and phosphates, silicates and ferric oxides/hydroxides [1]), and often allows obtaining, in physiological conditions, nanostructured materials exhibiting much better properties than artificial ones, with no need of high temperatures or high pressures for their synthesis [2]. Silicon, in particular, is the second most common element on Earth and biosilicification is the process by which inorganic silicon is incorporated into living organisms as silica [3]. Different eukaryotic organisms like sponges, radiolarians, higher plant and animals, are able to convert dissolved Si (DSi) into mineralized structures [4]. Diatoms in particular are able to synthesize nanostructured glass at room temperature starting from monosilicic acid ($Si(OH)_4$) dissolved in water [5], while most human common glass artifacts still need molten sand at temperatures over 1000 °C to be fabricated [2].

Diatoms are ubiquitous, unicellular micro-algae living in a large variety of genera and species both in the oceans and in freshwater [6]. Being responsible for about 20% of the global primary production and of 240 Tmol of annual biogenic silica precipitation [7,8], diatoms are one of the most influential organisms in terms of impact on the ecology and biogeochemistry of our planet. $Si(OH)_4$ uptake finally results in the generation of the frustule, an external, micro- and nano-structured porous

silica shell whose ordered morphology initially induced the first observer of diatoms (an anonymous English country nobleman of the early XVIII century [5,6]) to question if they were crystals or plants. Frustule silica structure is developed within a cellular compartment called silica deposition vesicle (SDV) [4,9] and its formation is mediated under strict genetic regulation by a series of proteins and other organic compounds (e.g., silaffins, frustulins, cingulins, long chain polyamines), which control and direct silica precipitation, growth and spatial distribution [10].

Frustules seem to fulfill at least four main functions: mechanical stability (the presence of pores and ridges lower the average stress concentration on the structure allowing the frustule to resist to pressures ranging from 1 to 7 N/mm^2, equivalent to 100–700 t/m^2 [11]); filtering of noxious agents (e.g., separation of nutrients from viruses) [12,13]; sinking speed lowering, allowing for a longer stay of diatoms near ocean surface and, consequently, a longer exposition to sunlight [14]; efficient coupling with sunlight to optimize photosynthesis [15].

Diatom cultures can be viewed as near-zero cost "living nanofactories", being able to produce at high rate and on a large scale three-dimensional nanostructures whose complexity can be hardly reproduced even by the most advanced lithographic techniques. It is not surprising, thus, that in the last 20 years a plethora of applications exploiting diatom frustules and their unique properties have been envisaged and tested in different fields such as optoelectronics [16], plasmonics [17], catalysis [18], biochemical sensing [19], solar energy harvesting [20], biomedicine and drug delivery [21], to name a few, all contributing to what we can define as diatom nanotechnology [22]. In many of these applications, frustule composition needs to be modified in order to obtain the desired functionalities. In general, frustule modification allows broadening the range of potential uses of the material.

In the present review article, the main physical and chemical techniques aimed at frustule modification are summarized, with indication of some of the relative applications that can be derived. The frontier of frustule modification is represented by the possibility to obtain, by means of the most recent genetic engineering techniques, mutants with a desired frustule morphology for a specific application. The first attempts to reach this goal are reviewed. In general, this overview is focused on intact frustules since we are interested in the exploitation of its complete morpholgy, geometry and characteristic simmetries. The use of diatomite (sedimentary powder derived by fossilized diatoms), e.g., in drug delivery and teranostics, deserves a deep, separate discussion that is beyond the scope of our study.

2. The Anatomy of the Frustule

Frustule is the characteristic feature of diatoms and one of the most representative examples of hierarchical organization in biomaterials, with levels of order extending from the nano to the microscale. The shape and dimension of frustules are species-specific, with sizes ranging from microns to millimiters. Nevertheless, some characteristics are common to all genera [6]. Frustules indeed always consist of an *epitheca* (see Figure 1) overlapping a *hypotheca* in a "petri-dish-like" arrangement. Every *theca* is formed by a valve and a series of lateral bands (girdle bands or *copulae*) connected along the margins. The full series of girdle bands form the so called *cingulum*. Both valves and *copulae* are characterized by the presence of regular, periodic or quasi-periodic arrangements of pores whose dimensions (from tens of nanometers to about one micron) depend on the considered species and on the position in the frustule. The valve indeed can be structured in a series of superimposed layers decorated with pores of different dimensions and spatial distributions. In Figure 2, some details of the ultrastructure of the frustule of a *Coscinodiscus* sp. diatom are shown. In particular, looking at the cross-sectional view of the single valve, we can distinguish an inner layer provided with chambers (the *areolae*) known as *foramen*; the roof of the *areolae*, called *cribrum*, characterized by a regular pattern of smaller pores; and, finally, an external membrane provided with even smaller pores known as *cribellum*.

The simmetry of the frustules allows distinguishing between two main classes: centric diatoms, mainly planktonic and characterized by round or polygonal valves, and pennate diatoms, mainly benthonic and commonly provided with bipolar, elongated valves.

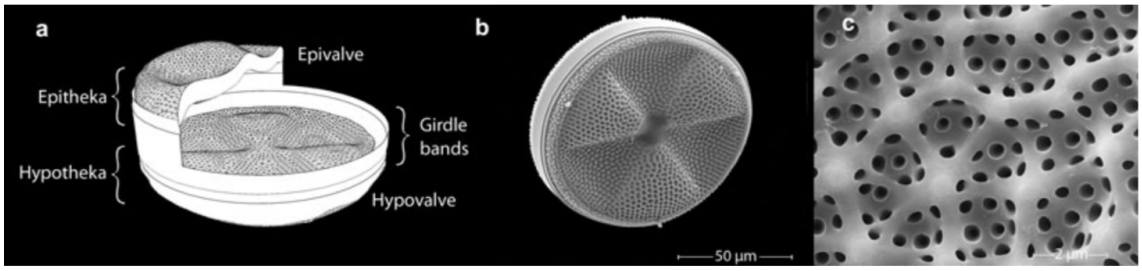

Figure 1. (**a**) 3D schematic model of an *Actinoptychus senarius* frustule with indication of the single components. (**b**) Scanning electron microscope (SEM) image of the whole frustule. (**c**) Detail of the valve. Reproduced with permission from Ref. [23].

In order to obtain a clean frustule, the organic content of the cell and the organic matrix that protects the silica wall have to be removed. Usually a treatment in hot acidic solutions (sulfuric acid, nitric acid, hydrogen peroxide or sodium dodecyl sulfate (SDS)/ethylenediaminetetraacetic acid) are used and followed by rinsing and centrifugation [24–26]. Recently, Gholami et al. [27] succesfully applied to frustule cleaning a method known as sono-Fenton (SF) process, based on the combination of Fenton process, which makes use of the reaction between ferrous ions and hydrogen peroxide to produce $^{\bullet}$OH radicals, and ultrasonic irradiation.

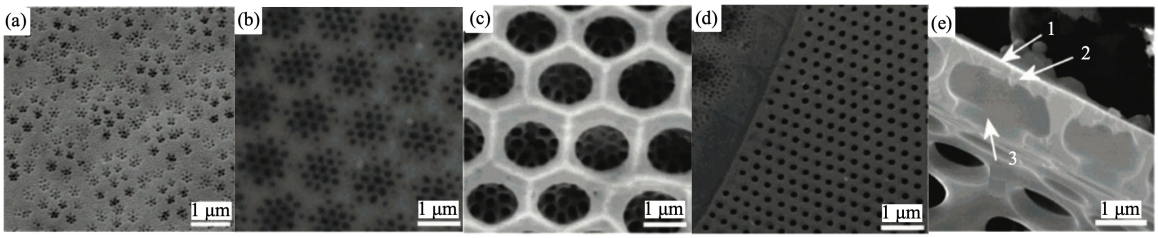

Figure 2. (**a**–**c**) SEM images of the different layers of a single valve of a *Coscinodiscus* sp. diatom frustule: cribellum (**a**), cribrum (**b**), and foramen (**c**). (**d**) a detail of the girdle band area; (**e**) sectional view of the valve. Arrows indicate : cribellum (1), cribrum (2), and the internal plate (3). Adapted with permission from Ref. [28]. Copyright 2007 American Chemical Society.

3. Frustule Modification: Techniques and Applications

3.1. Frustule Metabolic Doping

The possibility to insert semiconducting or metallic elements in dielectric nanomaterials in order to modify their morphological, photo- and electro-luminescent properties is of great interest in several fileds, e.g., in sensing, optoelectronics, solar energy harvesting, catalysis, and biomedicine [29]. In this context, diatom cultures can be viewed as potential biofactories for massive bottom-up production of hierarchical, nanostructured hybrid materials. An example is given by the metabolic insertion of germanium in *Pinnularia* sp. frustules as described in Ref. [30] and whose principle is schematized in Figure 3. In the first stage of the process, a diatom cell suspension is grown under silicon starvation, then silicon and germanium are co-added to the culture allowing the uptake of germanium by the dividing cells and its incorporation in the frustules of the newly divided ones. As long as the initial Si:Ge molar ratio is at least 14:1, no inhibition of cell division has been observed. By ion-coupled plasma (ICP) analysis, germanium resulted alloyed into the silica matrix of the frustule in the form of Ge-oxide nanoclusters or germananosilicate (Si-O-Ge) and not simply adsorbed or randomly precipitated onto the surface of the cells. Even though the overall shape of the frustule at the micron scale resulted unaltered after germanium metabolic insertion, geometry of the *areolae* was modified by the thickening of the frustule silica induced by germanium oxides. Metabolic insertion of germanium can thus represent a way to obtain controlled modification of the pore shape.

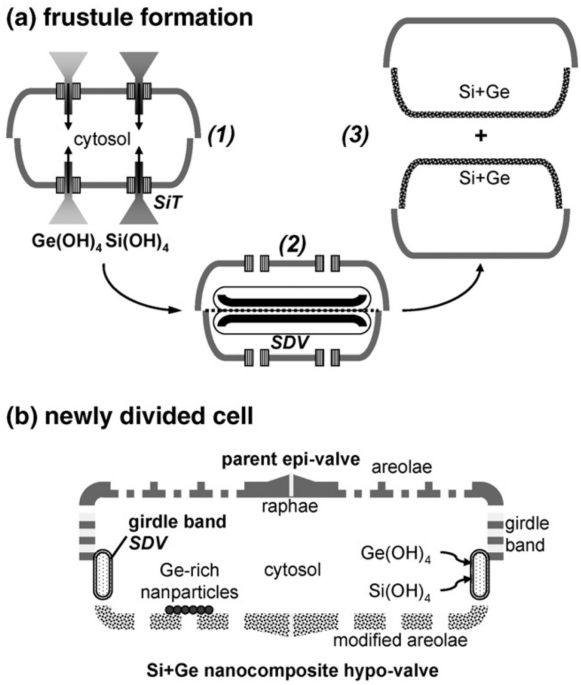

Figure 3. (**a**) Conceptual scheme for metabolic insertion of germanium into a diatom frustule: (1) uptake of Si and Ge by Si transporters (SITs); (2) valve development within the silica deposition vesicle (SDV); (3) cell division. (**b**) Simplified representation of the frustule of the newly-divided cell, showing intracellular Ge located in the new hypo-valve, Ge-rich nanoparticles, and the developing girdle band. Reproduced with permission from Ref. [30].

It is konwn that diatom biosilica is characterized by visible photoluminescence under UV excitation, with a peak in the blue sprectral range [31]. This is mainly induced by surface defects, including silanol groups (=Si-OH), and organic residuals incorporated in the frustule matrix [15,32]. *Pinnularia* sp. frustules containing metabolically inserted germanium are characterized by a more intense photoluminescence emission if compared to non-doped frustules [33]. Indeed, also Ge-O defects in amorphous silica are known to induce blue photoluminescence, which thus superimposes on that of diatom biosilica. Besides photoluminescence, Ge-doped frustules present also electroluminescence whose spectrum is characterized by narrow peaks consistent with the calculated resonance modes of the diatom frustule modeled as a photonic crystal (PhC) slab (for a wide treatise of photonic and optical properties of diatom frustules, refer to [15,34]). Conversely, the metabolic doping of *Coscinodiscus wailesii* frustules with nickel [35] resulted in quenching of the photoluminescence detected at 544 nm after excitation with blue light, probably due to overlapping of the biosilica emission spectrum with the asbsorption of the complexes formed by nickel ions within the hydrated frustule matrix. The modification of the optical properties of the frustule after nickel insertion, together with changes in its morphology (in particular the enlargement of the pores), allows one to consider diatom frustules as potential active component of an aquatic pollution sensing system.

A two-stages approach similar to the one described above for germanium was adopted by the same authors for the metabolic insertion of titanium [36]. At the end of the process, titanium is mainly localized as a nanophase surrounding the base of each frustule pore. The obtained biogenic titanate can be easily converted into nanocrystalline anatase TiO_2 by thermal annealing in air at 720 °C.

In recent years, diatom frustules-TiO_2 composites have been extensively tested and exploited to increase the efficiency of dye-sensitized solar cells (DSSCs) [20,37–40]. In a traditional DSSC, a photosensitive dye is bound to a photoanode comprised of anatase TiO_2 nanoparticles. When exposed to light, the dye absorbs photons and in its photoexcited state injects electrons into the conduction band of the semiconducting TiO_2. Finally, the electrons diffuse through the mesoporous titania layer

to the working electrode while the dye is regenerated by a liquid electrolyte [37]. In Ref. [20] titania was substituted by diatom frustules enriched with titania nanoparticles by means of plasma treatment (thus avoiding any linking agent usually exploited in silica functionalization). The high effective surface area of the resulting three-dimensional hybrid structures and the multiple scattering events induced by frustules pores ensure an enhanced interaction of the incoming light with dye electrons. After only three cycles of plasma treatment, an increase of conversion efficiency of about 30% with respect to conventional DSSCs has been achieved. A further improvement in efficiency (up to about 35%) and in the stability of the cell has been very recently obtained by replacing the liquid electrolyte by a gel polymer electrolyte and avoiding the use of volatile solvents for its preparation [39]. In this case the hybrid layers have been obtained by spin coating of a proper mixture of TiO_2 P90 powder and diatom frustules. An alternative way to obtain silica-titania nanostructured hybrids useful in DSSCs is of course given by metabolic insertion, as described in Ref. [38]. The authors also proposed a model for the realization of "living DSSCs" to generate electrical pulses aimed at the extraction of oil from diatom cultures without sacrificing the cells. Titania is metabolically inserted by the two-stage cultivation process described in [36] and the culture medium supplemented with an electrolyte and ruthenium dye as a photoactive dye. Electric pulses generated after exposure to light can fracture the frustule, causing lipid drops to ooze from the cells to the culture medium. The diatoms can heal their frustules when fed with nutrient media. The use of electric pulses has been tested for the extraction of proteins from *Chlorella vulgaris* and *Haematococcus pluvialis* microalgae, characterized by hard cell walls healed after a suitable incubation time.

Other metal and semimetal ions tested in metabolic insertion comprise aluminium in *Stephanopixis turris* [41], with potential applications in catalysis; europium in *Navicula* sp. [42], which gives frustule biosilica photoluminescent properties with red light emission (614 nm) after excitation at 394 nm; calcium in *Thalassiosira weissflogii* [43] with potential applications in biomedicine of the obtained hybrid frustules as substrates for fibroblasts and osteoplasts growth; tin in *Synedria acus* [44], which decreases the mechanical strength of the frustule; zirconium in *Phaeodactylum tricornutum* [45] for applications in electrochemical sensing aimed at detection of methyl parathion.

Metabolic incorporation of rhodamines into diatom frustules by means of *in vivo* fluorochromation has been exploited by Kucki et al. [46,47] in order to study how frustule quasi-periodic nanostructure acts on the emission of an embedded dye, in an analogy with the study of the interaction between a PhC and an integrated emitter (e.g., a quantum dot) [48,49]. This approach is also efficient at following the biomineralization process of frustule formation, as an alternative to more traditional tools for labeling silica in living diatoms. The authors show how, even after prolonged exposures to Rh 19 (up to eight weeks) and for a wide range of dye concentrations in culture medium, cells were still capable of reproduction with no observable morphological aberrations of the wall [47]. Furthermore, the dye resulted incorporated in both *thecae* (see Figure 4).

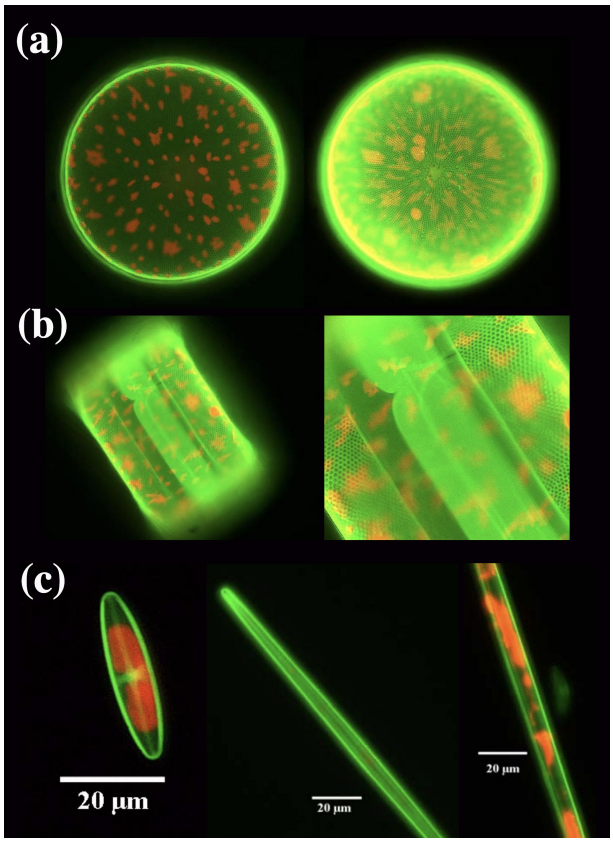

Figure 4. (**a**) Fluorescence of a living *Coscinodiscus wailesii* diatom grown in 1 µM (**left**) and 10 µM (**right**) concentration of Rh 19. Red autofluorescence of choloroplasts is also visible. Valve diameter ≃220 µM. (**b**) Lateral view (**left**) and relative detail (**right**) of a living *C. wailesii* diatom cell after several division cycles. The frustule as a whole results fluorescent (both *techae* are stained). Diameter of the valve ≃200 µM. (**c**) Examples of pennate freshwater diatoms grown in a Rh 19 doped culture medium. (**a**) reproduced with permission from [47]. (**b**,**c**) reproduced with permission from [46].

Dye photoluminescence is in general affected by the regular structure of the frustule and its photonic properties [50]. Indeed, as widely reported in literature [15,34,51–58] and already mentioned before, diatom frustule valves and girdles can be viewed as PhC slabs made of a regular pattern of holes in a silica matrix. When properly dimensioned, PhC slabs are able to couple and guide light of specific wavelengths (resonant modes) and/or to inhibit the propagation of light whose wavelength lies in the so-called photonic band-gaps (PBGs) [59,60]. Frustule pore patterns are thus able to modulate the light emitted by a dye deeply embedded in the silica matrix after in vivo, metabolic incorporation. In Ref. [50], Ragni and coworkers made use of a fluorophore provided with a phenyleneethynylene conjugated backbone and a triethoxysilyl functional group (PE-Syl) in order to metabolically dope a *Thalassiosira weissflogii* culture. The phenyleneethynylene backbone was selected for its high photoluminescence efficiency and photochemical stability and its low cytotoxicity, while the triethoxysilyl functional group was introduced to allow the uptake of the PE during the silicification process, normally based on orthosilicil acid $Si(OH)_4$ as inorganic silicon source. No significant toxic effect of PE-Syl was observed up to 96 h after its inoculation, when the cell density reached a plateau value. Even after removal of the organic content of the cells, Raman spectroscopy, time of flight-secondary ion mass spectrometry (ToF-SIMS) and Fourier transform infrared spectroscopy (FT-IR) measurements still confirmed the presence of PE-Syl inside the biosilica matrix of the frustules. The spectral content of the emitted photoluminescence of incorporated PE-Syl was strongly affected by the frustule PBGs because of the interaction between valves and girdles transmittivity and dye emission spectrum. Light filtering and trapping in solar energy harvesting,

bio-based random lasers and local metrology are some of the possible applications that can exploit the interaction between photonic properties of frustules and photoluminescence emission of embedded dyes [50].

3.2. Frustule Metalization for Applications in Plasmonics

Metallic–dielectric interfaces excited with optical radiation at specific wavelengths support the propagation of surface palsmon polaritons (SPPs), determined by collective oscillations of conducting electrons. In case of metallic nanoparticles or nanostructured metallic substrates the plasmonic field is strongly confined, giving rise to localized surface plasmons (LSPs) [61]. One of the most widespread applications of plasmonics is surface enhanced Raman spectroscopy (SERS), where LPs are exploited to enhnance the Raman emission of molecules in proximity of the metallic nanostructures, compensating the low cross section characteristic of the process [62]. The enhancement factor (*EF*) is defined as:

$$EF = \frac{I_{SERS}/N_{surf}}{I_{RS}/N_{vol}}, \quad (1)$$

where I_{SERS} and I_{RS} are SERS and Raman intensities, N_{surf} is the average number of molecules adsorbed to the metallic substrate in the scattering area for the SERS measurements, and N_{vol} represents the number of molecules present in bulk in the scattering volume for spontaneous Raman scattering measurements.

Two main approaches are usually followed in the realization of SERS substrates. On one hand, bottom-up chemical synthesis allows obtaining a plethora of metallic nanoparticles such as colloidal silver and gold nanoparticles [63], silica-coated metallic nanoparticles [64], monolayers of aligned metallic nanowires [65], metallic nanoprisms, nanocubes, nanostars, and nanosheets [66–69], all ensuring high values of the enhancement factor but lacking in tunability, robustness and reproducibility. On the other hand, top-down nanolithographic techniques are used in the fabrication of plasmonic nano-antennas arrays [70,71], subwavelength gold gratings [72], dielectric photonic crystals coupled with metallic nanoparticles [73], optical fibers provided with nanostructured, metallized facets [74], nanostructured metallic fishnets [75], and three-dimensional hollow nanostructures with tunable geometries [76], to name a few. Even though these solutions guarantee high reproducibility in the aquisition of the spectra, generally result expensive and prohibitive for large-scale production and routine practical applications.

Being formed by a complex, intricate but still regular dielectric three-dimensional micro- and nano-structure, it is straightforward to hypothesize that diatom frustules, if properly metalized, are able to trigger plasmonic effects, presenting the additional but not negligible advantage to avoid both the loss of reproducibility proper of traditional bottom-up approaches and the prohibitive cost, complex fabrication and hard feasibility in mass production typically affecting top-down techniques. One of the the first attempts to use diatom frustules as SERS substrates consisted in the realization of silver replicas of *Synedra* sp. and *Thalassiosira* sp. valves by chemical removal of silica after frustule covering with evaporated silver [77]. The resulting metallic nanostructures, when used as SERS substrates, allowed obtaining enhancement factors up to $\sim 10^6$ for rhodamine as analyte and assuming a 100% covering of the dye on the silver shell. Another approach used to metalize diatom frustules consists of the chemical attachment of metal nanoparticles to diatom biosilica, thus promoting the coupling of the guided-mode resonances supported by the valves to the LPs of the nanoparticles. The resulting hybrid photonic-plasmonic modes ensure high quality factors of the local electric field. Ren et al. [78] obtained silver nanoparticles self-assembly to amine-functionalized *Pinnularia* sp. valves and tested the resulting hybrid nanostructures as SERS substrates. Under non resonant condition and over a concentration interval of 10^{-7}–10^{-4} M, an increase in EF up to 12 times has been observed comparing the acquired spectra of rhodamine 6G dropped on valves and on a reference glass slide, respectively, both conjugated with silver nanoparticles. The same hybridization process has been exploited for the same diatom species in the development of a SERS-based sandwich immunoassay

system aimed at the detection of antibody–antigen interaction [17]. In this case, the silver nanoparticles not only provide SERS enhancement, but are also used as substrates for antibody attachment. The experimental results proved that a detection limit down to 10 pg mL^{-1} can be achieved, which is two orders of magnitude better than the one obtainable by the corresponding flat SERS substrates. A similar sandwich structure has been used for interleukin 8 (IL-8) detection in blood plasma, starting by the functionalization of *Pseudostaurosira trainorii* diatom frustules with gold nanoparticles conjugated with DTNB as Raman reporter and with specific antibodies as bioprobes (see Figure 5) [79].

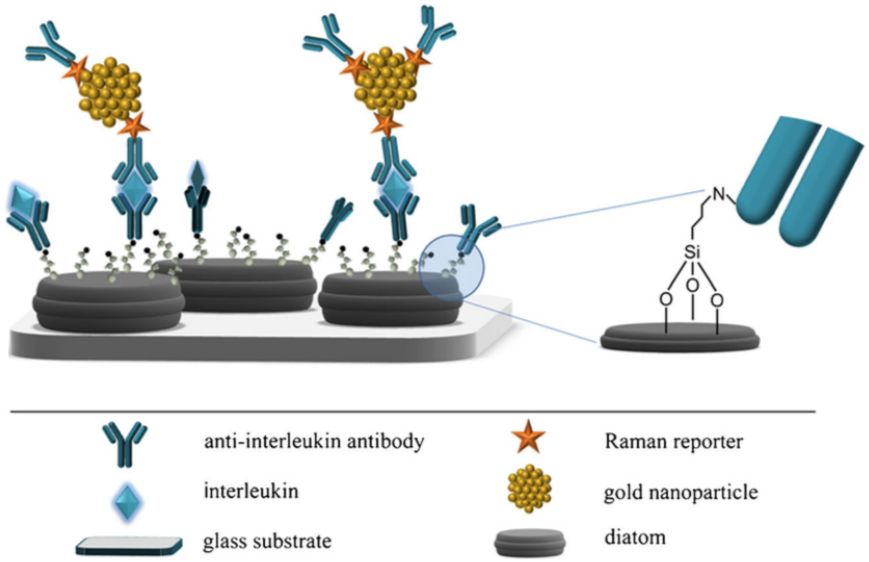

Figure 5. Schematic representation of the SERS immunoassay described in Ref. [79], with indication of the single elements of the sandwich structure. Antibody immobilization, interleukin capture and a detail of the link between the frustule and the bioprobe through an amino group are also illustrated. Reproduced with permission.

Gold nanoparticles do not present significative oxidation, which usually affects silver. The experimental results showed an improved detection limit in comparison to the traditional enzyme-linked immunosorbent assay (ELISA). In particular, the detection limit for IL-8 in human blood plasma was found to be 6.2 pg mL^{-1} versus 15.6 pg mL^{-1} obtained by ELISA, while it equals 2.5 ng mL^{-1} when using a glass-based SERS immune substrate.

Certainly the most straightforward and simple way to obtain a diatom-based SERS substrate is by thermal evaporation of metal without any subsequent chemical removal of the biosilica. The choice of the species is also crucial since a peculiar frustule morphology and geometry can represent the optimal solution for a specific application. An example is described in Ref. [80], where uniform thermal deposition of gold on valves of *Pseudonitchia multistriata* allowed the realization of SERS substrates for the efficient analysis of biochemical composition of cell membranes, in particular of red blood cells (RBCs) and B-leukemia REH cells. *P. multistriata* valves are provided with a vertical, extruded side edge (see Figure 6b) which ensures an optimal interaction with cells avoiding steric hindrance. SERS signals from the membrane, with no interference from other cellular components (e.g., hemoglobine in the case of RBCs and nuclear components in the case of leukemia cells) are fundamental in the assessment of several pathologies. In particular, *P. multistriata* frustules represent an example of natural *supergrating*, where different periodicities (see Figure 6a) interact optimizing the coupling with external optical radiation. When tested on a self-assembling biphenyl-4-thiol (BPT) monolayer (which uniformly covers the valve with a packing density of four molecules per nm^2) and with a nominal thickness of 40 nm of gold deposited onto the valve, an EF of $(4.6 \pm 0.9) \times 10^6$ is reached. A comparison between BPT spectra acquired onto the valve and outside the valve is reported

in Figure 6d. Furthermore, the authors envisage the use of free-standing, metalized *P. multistriata* frustules within a microfluidic system in order to obtain mobile, optical driven SERS microsensors able to be dragged toward the target cell.

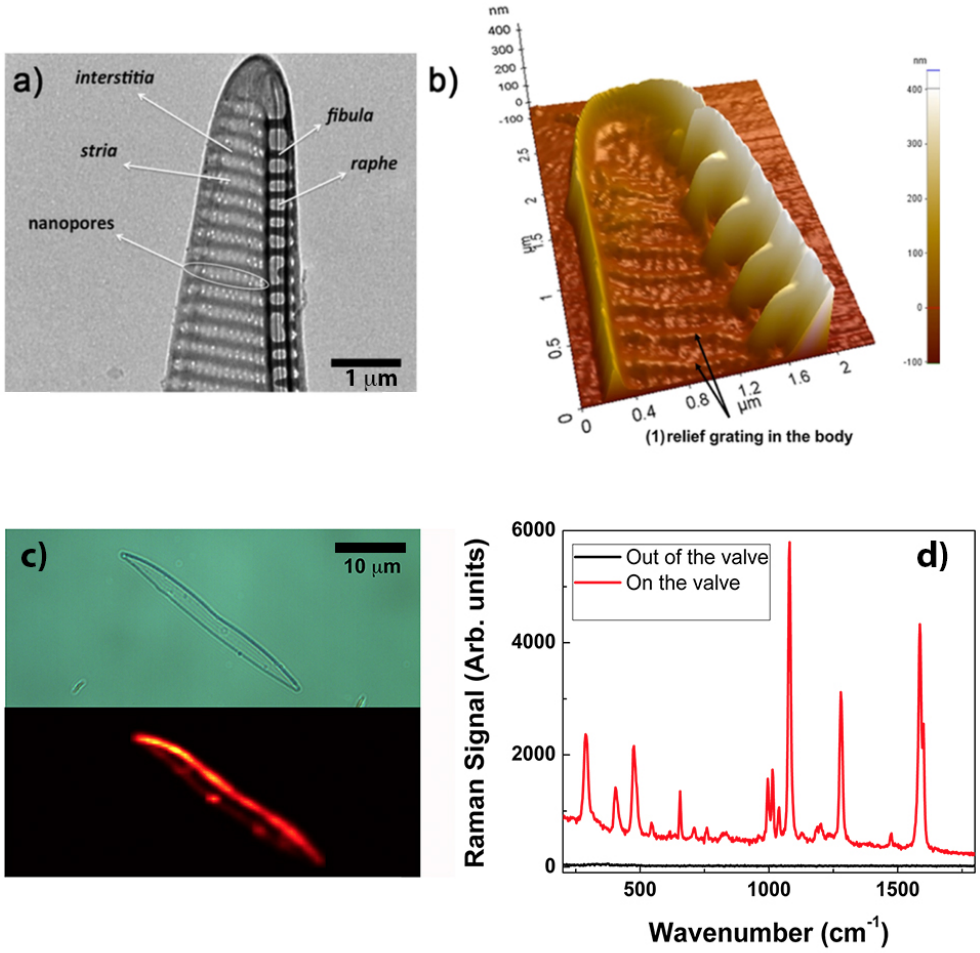

Figure 6. (**a**) Transmission Electron Microscopy (TEM) image showing the details of a *P. multistriata* valve with indications of its characteristic features. Several periodic subpatterns, whose overall interaction provides an efficient coupling with incident optical radiation, can be identified. (**b**) Atomic Force Microscopy (AFM) scan of a metalized valve showing its 3D morphology, in particular the extruded edge wall with its peculiar blade profile. (**c**) Optical image and relative Raman map of a single metalized valve covered with a biphenyl-4-thiol (BPT) monolayer used to estimate the EF. Most of the signal comes from the lateral, extruded edge. Gold thickness: 40 nm. (**d**) BPT average spectra outside (black) and on (red) the metalized valve after excitation at 785 nm. (**a**,**b**) reproduced with permission from Ref. [80]. Copyright 2018 American Chemical Society.

A similar concept is at the basis of the work of Sivashanmugan et al. [81], where multiscale hierarchical mesocapsules have been obtained starting from in-situ growth of silver nanoparticles onto *Pinnularia* sp. frustules. The bio-derived mesocapsules can easily flow inside a microfluidic channel and reach an interrogation site. The combined effect of high density of embedded nanoparticles, photonic crystal-induced enhancement of the plasmonic field, efficient analyte capture by the frustule porous matrix, and effective mixing with analyte in the microfluidic channel allowed reaching single molecule detection for Rhodamibe 6G and a detection limit of 1×10^{-9} M of benzene and chlorobenzene compounds in tap water with near real-time response.

In addition to SERS, other plasmonic effects can be induced by a suitable metalization of diatom frustules. Fang et al. [82] obtained gold replicas of *Coscinodiscus asteromphalus* valves by means of a combined process, comprising an amine-amplifying surface functionalization followed by a rapid, electroless gold deposition. A final selective removal of the underlying silica by dissolution in a HF solution allowed yielding freestanding gold structures that retained the geometry and morphology of the starting valves. These replicas showed transmission maxima and refelction minima at infrared wavelengths that cannot be found in the starting diatom silica valves nor in flat non-porous gold films used as references. This extraordinary optical transmission (EOT) effect has been ascribed, as confirmed by numerical simulations based on a surface plasmon interference model introduced by Pacifici et al. [83], to the combined effect of the periodic hole pattern inherited by *C. asteromphalus* valve and the involved gold chemistry, which induces the generation of surface plasmons and consequent interference with incoming light. Surface plasmon-mediated EOT usually finds applications in integrated optics and in chemical and biological sensing.

3.3. Fustule Functionalization for Protein Immobilization

Immobilization of proteins onto a solid support material allows improving their functionality by stabilizing their native conformation, which is of great benefit in several applications like catalysis, sensing, and drug delivery [84]. Diatom biosilica, in particular, offers several advantages if used as support material: its porosity, characterized by high values of specific surface area (up to 220 m^2 g^{-1}), provides a large capacity for binding proteins and a very effective interaction with several adsorbates [53]; the size of frustule pores is large enough to allow for the incorporation of protein molecules, which have an equivalent hydrodinamic diameter of the order of nanometers [85]; its high chemical and mechanical stability and its hydrophilic properties allow for hydrogen bonds and electrostatic interactions with proteins; its transparency in a wide interval of the visible and infrared spectrum make it possible to analyze the immobilized proteins by optical spectroscopy; finally, its biocompatibility allows for in vivo applications.

Among the possible in vitro techniques aimed at protein immobilization onto diatom biosilica, the most efficient are those based on the introduction of chemical functional groups able to irreversibly attach proteins to the hydrogenated silica frustule through covalent binding. Indeed silanol (≡Si-OH) and silanolate (≡Si-O^-) groups on the frustule surface are not able to directly form stable covalent bonds with protein molecules and further chemically reactive functional species have to be introduced as cross-linkers. Townley and co-workers [86] silanized *C. wailesii* frustules using the alkoxysilane 3-aminopropyltrimethoxysilane (APS) followed by N-5-azido-2-nitrobenzoyloxysuccinimide (ANB-NOS) as crosslinker in order to permit covalent bonding with anti-IgY (IgY: immunoglobulin Y) after exposure to UV light (see Figure 7). Conjugation with secondary antibody (horse radish peroxidase HRP) was verified by immunoblot chemiluminescence. Furthermore, in order to avoid multiple attachment sites via the amine groups with consequent distortion of the moiety, the authors tested a second method which exploits the carbohydrate side chains of the antibody through the oxidation of the hydroxil groups of the sugar residue on its Fc region to form aldehydes.

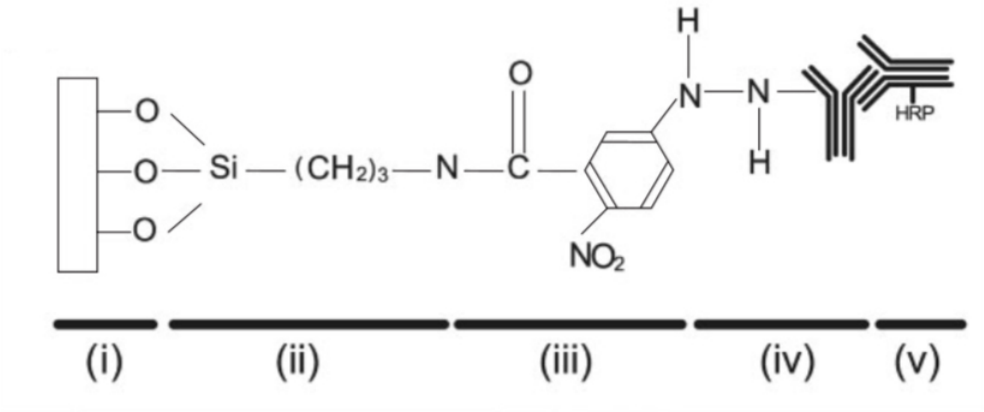

Figure 7. Schematic representation of a functionalized biosilica surface obtained by one of the methods described in Ref. [86]. (**i**) frustule surface; (**ii**) 3-aminopropyltrimethoxysilane (APS); (**iii**) N-5-azido-2-nitrobenzoyloxysuccinimide (ANB-NOS); (**iv**) primary antibody; (**v**) secondary antibody with horse radish peroxidase (HRP) conjugate. Adapted with permission from Ref. [86].

In Ref. [87] De Stefano et al. applied, for the same diatom species, a functionalization method usually implemented in chemical modification of oxidised porous silicon [88] and based on aminopropyltriethoxysilane (APTES) for silanization and glutaraldehyde (GA) as cross-linker. The obtained modified active surface is able to attach also DNA single strands other than proteins [89]. In the reported study, murine monoclonal antibody (MoAb) UN1, characterized by a specific reactivity with human thymocytes [90], has been used as molecular bioprobe to be attached to *C. wailesii* frustule. Futhermore, Protein A from *Staphilococcus aureus* has been used as a biospecific spacer arm in order to properly orient MoAb. Every single step of the functionalization process has been verified by means of FT-IR spectroscopy and rhodamine labelling of bioprobes has been used to test the quality of the functionalization process by means of fluorescence microscopy. The same protocol involving the use of APTES and GA has been used by Bayramoglu et al. [91] for tyrosinase immobilization onto pennate diatom frustules. The obtained active biosilica was tested in degradation of phenolic compounds (phenol, para-cresol and phenyl acetate) in a batch system. The same authors reported lipase immobilization onto *Scenedesmus quadricauda* frustules after bromoacetylation of the silanol groups and subsequent polymerization of 2-choloethyl acrylate (CEA). Finally, the terminal chloride groups were reacted with ethylene diamine to introduce amino groups that were cross-linked to lipase using GA. The obtained modified frustules were used in biodiesel synthesis from algal oil with a conversion efficiency of about 83% [92].

The combination of frustule photoluminescence properties with the ability to covalently bind bioprobes to frustule surface allows obtaining very efficient diatom-based optical biosensors [93–96]. It has been demonstrated, indeed, that the spectral characteristics of the frustule photoluminescence emission are strongly affected by the chemical composition of the environment [97–99], making it possible to obtain an efficient optical transducing mechanism also for the detection of bioprobe-target recognition events. Rorrer and co-workers [100] functionalized *Cyclotella* sp. frustules with amine groups by reaction with APS, bissulfosuccinimidyl suberate (BS3) as crosslinker, and rabbit IgG antibody as anchored bioprobe, obtaining an efficient, label-free photoluminescence-based biosensor for immunocomplex detection. Amine and antibody functionalization steps have been verified by means of epifluorescence imaging after suitable labeling of the free amine sites and goat anti-rabbit IgG antigens, respectively. After immobilization of nucleophilic IgG, the intrinsic blue photoluminescence of diatom biosilica resulted enhanced by a factor of six, while immunocomplex formation with anti-rabbit IgG further increased the peak photoluminescence intensity of at least a factor of three. Photoluminescence enhancement is ascribed to electron donation of the nucleophilic immunocomplex to non radiative defect-sites of diatom biosilica. In Figure 8, the characteristic dose-response curve of the sensor is reported with indication of the binding constant.

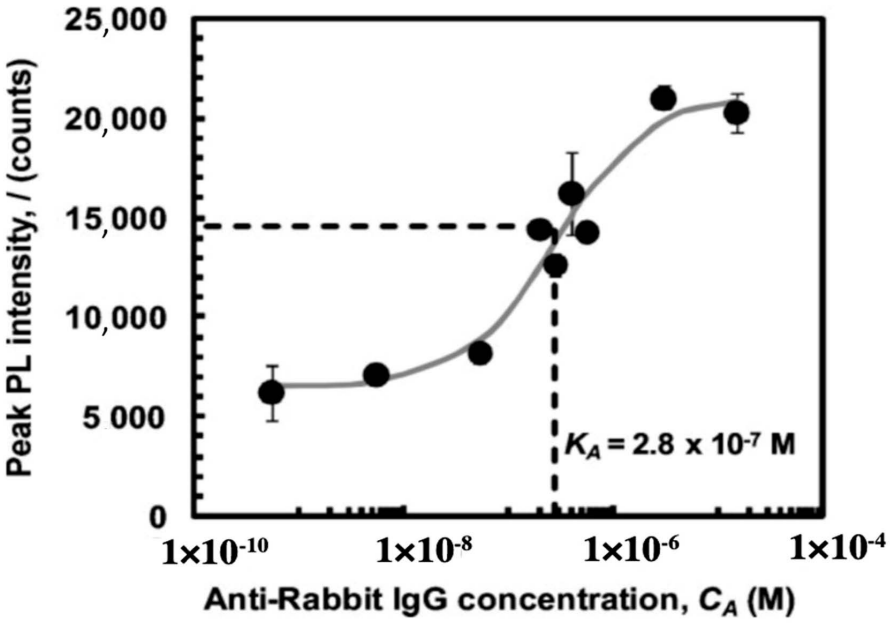

Figure 8. Dose-response curve of the label-free photoluminescence-based biosensor described in reference [100]. Binding constant is also reported. Reproduced with permission.

3.4. Frustule Replicas

One of the main advantages represented by the use of diatom cultures in nanotechnology is the near-zero cost availability of complex, three-dimensional micro- and nano-structures able to self-replicate at high rates with a remarkable reproducibility, giving rise to complex geometries and architectures hardly feasible even by means of the most advanced lithographic techniques [53,80,94]. Nevertheless, silica may be not the ideal choice for a specific application. In addition to metabolic insertion of ions in culture medium, which does not allow for the complete substitution of silica with other materials, other methods have been introduced through years aimed at the realization of accurate frustule replicas in different materials. High-refractive index frustule replicas can, for example, support wide and complete PBGs [53]. A case of metallic replica of a frustule has been already reported in Section 3.2, but other examples deserve to be mentioned.

Losic and coworkers [101] developed a low-cost, 2-step process based on a soft polymer mold in polydimethylsiloxane (PDMS) and subsequent transferring of the pattern from PDMS onto a hard photo-curable polymer to obtain a positive replica of the frustule (see Figure 9a). Actually the process can be applied to other kind of materials and the valve porous patterns can be tranferred to gels, precursors to ceramics and carbons, luminescent phosphors, salt and colloids. Depending on the starting diatom species, a huge variety of patterns can be transferred. The obtained replicas can find application as complex optical elements, masters for nanofabrication, biosensing devices and nanoreatcors.

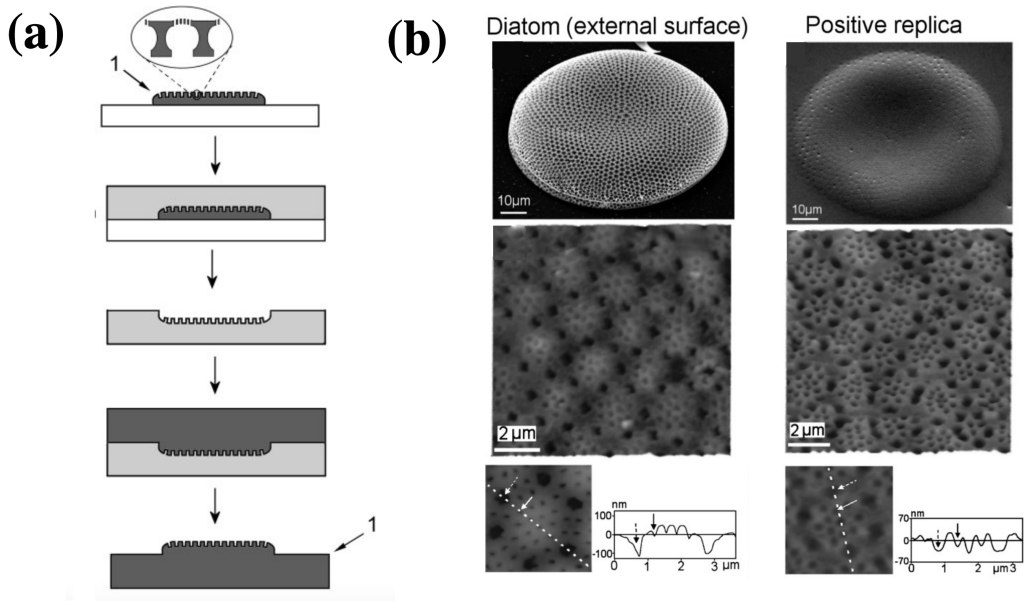

Figure 9. (**a**) Schematic representation of the replica molding process described in Ref. [101]: a single valve is transferred into a PDMS matrix (negative replica) which in turn is replicated into mercaptol ester type UV curable polymer (NOA60), thus leading to a positive replica. (**b**): SEM and AFM images of a single *Coscinodiscus* sp. valve (left column) and NOA 60 replica of its cribrum (right column). Adapted with permission.

Silicon replicas of *Aulacoseira* frustules have been synthesized by Bao et al. [102] making use of a shape-preserving magnesiothermic reduction. In the first stage of the process, MgO/Si replicas are obtained starting from a frustule-bearing steel boat and magnesium granules placed for 2.5 h in a furnace preheated at 650 °C, according to the following reaction:

$$2\mathrm{Mg(g)} + \mathrm{SiO_2(s)} \rightarrow 2\mathrm{MgO(s)} + \mathrm{Si(s)} \quad (2)$$

where (g) and (s) stand for gaseous and solid state, respectively. Subsequent treatments in HCl and HF solutions allowed the selective dissolution of magnesia. The chemical and structural composition of the obtained replicas have been scrutinized aby FT-IR spectroscopy, Energy Dispersive X-Ray Analysis (EDX) and X-ray diffraction (XRD). Silicon resulted as a crystalline phase characterized by an average crystallite size of 13±2 nm. Finally, since the obtained silicon frustules were charaterized by an impedence strongly dependent on the chemical composition of the environment, they have been succesfully tested as NO(g) sensors.

Pan et al. [103] obtained graphene replicas of *Aulacoseirea* sp. frustules by means of chemical vapor deposition (CVD) of methane followed by dissolution of the silica in hydrofluoric acid. During CVD, hydrocarbon species infiltrate into all the frustule surfaces, including the inner ones, and form a continuous graphene coating that retains the frustule shape in all its details. Since graphene is highly transparent to electron beams, this allows the visualization of the internal morphology of valves and girdles, revealing the complex, interconnected nanotubes linking their different layers.

Mn–iron hydroxide hybrids have been obtained starting from diatom frustules by Li et al. [104]. The three-step process starts with a hydrothermal treatment in a $KMnO_4$ solution, which promotes the formation of a MnO_2 layer onto the diatom valve. Then, a $FeSO_4{\cdot}7H_2O$ solution is used to promote MnO_2 tranfert into iron hydroxide through redox reaction between Fe^{2+} and MnO_2. In the last step, silica is removed by a KOH solution etching. The obtained hybrid replicas preserve the starting frustule shape and morphology (as confirmed by SEM characterization) and their chemical composition has been scrutinized by EDX spectroscopy and mapping. The authors analyzed a series of differently tuned materials (MnFeOx, Fe(OH)x, and FeOOH) and the corresponding replicas have been tested

as electrodes in asymmetric supercapacitors (MnO_2 replicas resulted to behave as positive electrodes while FeOOH replicas as negative electrodes). The enlarged surface area and increased active sites in contact with the electrolyte improve the electrochemical properties of the tested electrodes.

Even though not related to frustule modification, a few biomimetic approaches in the fabrication of diatom shell replicas deserve to be mentioned. Xu et al. [105] developed a technique based on direct ink writing (DIW) [106] and subsequent exposition to silicic acid in order to obtain 3D replicas of *Triceratium favus* Erhenberg (traingular-shaped) and *Arachnoidiscus ehrenbergii* (web-shaped) frustules (see Figure 10), starting from concentrated polyamine-rich ink. The biomimetic silification process is carried out by immersion of the polymeric scaffolds in aqueous phosphate buffered silicic acid solutions. The obtained replicas can be easily converted to other materials such as MgO or titania through a halide/solid displacement reaction.

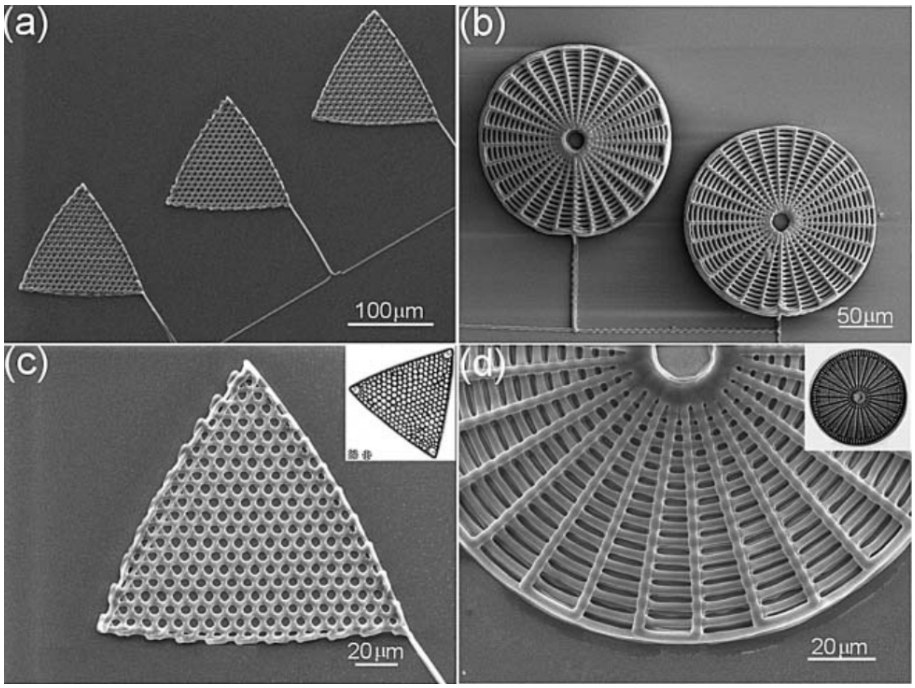

Figure 10. SEM images of polyamine-rich scaffolds assembled by direct ink writing and reproducing the morphology of a *T. favus* (**a**) and a *A. ehrenbergii* **(b)** diatom valve. Magnification views are reported in (**c**,**d**). Reproduced with permission from Ref. [105].

Ceramic titania artificial photosynthetic systems mimicking the hierarchical morphology of *C. wailesii* multi-layered valves have been fabricated by a combination of electron beam lithography (EBL) and nanoimprint lithography (NIL) [107]. When loaded with gold nanoparticles (AuNPs), the titania replicas present a marked absorption peak in the 300-420 nm spectral region. At the end of the CO_2 photoreduction process, the generation rates of CO and CH_4 were considerably incremented respect to the case in which AuNPs-loaded TiO_2 powder was used as photocatalyst sample.

3.5. Frustule Genetic Modification

Diatom biosilica is a hybrid material which consists of amorphous silica and several organic compounds. The formation of the diatom frustule structure is coordinated and dependent by both silica polymerization in the SDV and self-assembly processes that involve different proteins and molecules [5,9,10]. In 1996, Kröger and co-workers identified and isolated the first protein from the frustule, that they called frustuline [108]. Over the past 25 years, through biochemical analyses and -omics studies, many other proteins and organic compounds involved in frustule formation and scaffold have been identified and partially characterized (e.g., long-chain polyamines, silaffins, silacidins, cingulins, and polysaccharides) [10].

The process of frustule formation is under the control of a genetic, species specific, finely tuned mechanism which, at each division, is transmitted from the mother to the two derived daughter cells. The extraordinary precision and frequency with which this mechanism occurs has always fascinated and intrigued biologists and different models have been proposed. However, to date none of them is able to explain biosilica morphogenesis in its entirety [109]. Indeed, there are still many components of the process that should be clarified, such as how this higher-order structure is formed and what are the exact spatial and temporal mechanisms that are imparted on the process. The manipulation of the silification process and the alteration of the architecture of the frustule by genetic modification is challenging and can be an effective and powerful approach to address those questions [34]. In addition, understanding and modifying the process of biomineralization in diatoms might result in a powerful tool for a wide variety of nanotechnological applications [110].

Compared to other organisms, the genetic engineering of diatoms is still in its infancy. Genetic reporter systems to study gene expression and regulation and spatial localization of proteins [111], modulation of gene expression methods, overexpression [112], gene knockdown [113], knockout, tailored TALEN endonucleases [114] and the CRISPR/Cas9 system [115] are now available also for these microalgae, allowing genetic modifications and the generation of mutated strains [116]. These molecular tools allow to investigate the function and the role of the proteins involved in cell wall biogenesis and their properties [117,118]. *Phaeodactylum tricornutum* and *Thalassiosira pseudonana* are the two molecular model species, since *P. tricornutum* is characterized by fusiform cells with a cell wall poor in silica [119], while the centric *T. pseudonana* has been developed as a model species to study the formation of silica cell wall [120]. More recently, *Cylindrotheca fusiformis* is considered as well a model for silicification research [116].

In this section, we summarize up-to-date reports about the genetic engineering applied to diatom frustules, aimed at the characterization of the involved genes and the derived effects on the frustule formation, morphology, function and functionalization with implications for potential nanotechnological applications (see Table 1).

Table 1. Summary of the main model species used for frustule characterization with indication of the studied genes, encoded proteins and employed methods.

Species	Genes or Related Proteins	Method	Reference
T. pseudonana	Silicic acid transporters (SITs 1,2,3).	Gateway technology for GFP fusion proteins. RNAi and antisense knockdown. Target mutations.	[121] [122]
	Incorporated antibody-binding protein domains.	LiDSI-based method (live diatom silica immobilization).	[123]
	SAP1-2-3 (Silicalemma Associated Proteins).	Gateway technology for GFP fusion proteins. RNAi and antisense knockdown.	[120]
	Silacin-1 (Sin-1).	Cloning technology for GFP fusion proteins. CRISPR/Cas9-based approach.	[124] [118]
	Silaffin-1 (Sil1) and cingulin genes family (CinY1, -2,-3,-4 and CinW1, -2, -3).	LiDSI-based method (live diatom silica immobilization).	[1]
C. fusiformis	Silaffin-1 (Sil1) (R5 peptide post-translational modifications).	*E. coli* expression system for the recombinant production of R5.	[125]
C. cryptica	ID g20669 (Sin1 homologue).	Cloning technology for GFP fusion proteins.	[109]

One of the earliest examples of genetic engineering-based approach in the study of frustule biogenesis has been reported for *T. pseudonana* by Shrestha and Hildebrand in 2015 [121]. The authors, using Gateway technology for GFP fusion proteins and antisense RNA and RNA interference (RNAi) approaches, determined the spatial localization and the regulatory and signaling role for the individual silicon transporters genes (SITs). The obtained results confirm the primary and already known role of these proteins in the silicon uptake from the environment into the cell but, unexpectedly, demonstrated further specialization of the SITs as sensors of cellular silicic acid levels that might elicit

and control cell wall formation and division processes. Afterwards, Knight et al. [122], in order to shed light on the molecular mechanisms of silicic acid transport, developed a fluorescence method to characterize more in detail the kinetics parameters of the SITs and demonstrated, through protein mutagenesis approaches, that the conserved four GXQ amino acid motifs plays an essential role in SITs function.

Transcriptome analysis in *T. pseudonana* cells has enabled the identification of different genes potentially involved in silica formation [126]. In particular, the study identified a set of genes, named Silaffin Like Response Genes (SLRGs) and in 2017 Tesson and co-authors identified and characterized a subset of three related new proteins, conserved in other diatom species as well [120]. Using the same approach of Shrestha and Hildebrand [121], the authors generated mutants expressing C-terminal GFP fusion proteins to determine their spatial sub-cellular localization. The results indicate an association of these proteins with the silicalemma (the membrane surrounding the SDV), and, for this reason, they named the family Silicalemma Associated Proteins (SAPs 1, 2 and 3). To further investigate their role during cell wall formation, the authors, starting from the results of spatial localization, generated knock down lines by antisense RNA and RNAi methods for two out of three genes, TpSAP1 and TpSAP3. The knock down lines were molecularly analyzed and the frustule architecture phenotypically characterized. Interestingly, the valves of knock down lines showed altered pattern morphology compared to the control wild type cell. In detail, the mutants have an approximately two fold bigger cell volume and a mislocated pattern center, but in general exhibit the same biosilica morphology than the wild type [120]. The reported results represent one of the first evidence that demonstrates that the ability to manipulate and modulate the expression level of one of the genes involved in the biosilification process is sufficient to generate a consistent phenotypic change in silica structure. In 2017, Kotzsch and colleagues discovered and determined the spatial localization, in *T. pseudonana*, of the first membrane protein located in SDVs, named Silicanin-1 (Sin1), highly conserved in all diatoms and that, in combination with long-chain polyamines, promote silica formation from silicic acid in vitro [124]. Later on, thanks to the advent of genome editing in diatoms, with the improvement of CRISPR/Cas9 precision technology, Gorlich and collaborators generated Sin1 knockout mutants in *T. pseudonana* [118]. The phenotipical and mechanical performance of the frustule of the knockout mutants enable to confirm the previous function of the protein in promoting silica formation.

Diatom shells are excellent natural porous materials for possible uses in nanotechnology such as drug delivery [22] and, with this aim, Delalat and co-workers [123] genetically modified *T. pseudonana* to display an IgG-binding domain of protein G on the biosilica surface, enabling attachment of cell-targeting antibodies trought a genetic method termed living diatom silica immobilization (LiDSI). The method, introduced by Kröger and co-workers [127,128], consists of the introduction of a recombinant gene encoding for an artificial protein formed by the desired enzyme or receptor protein fused to a protein of the organic matrix of the SVD (see Figure 11). In Ref. [123] the authors, for the simultaneous attachment of antibodies and hydrophobic drug molecules to diatom biosilica, used for the first time this genetic method to incorporate an immunoglobulin G (IgG)-binding domain of protein G19, named GB1, into the biosilica of the diatom *T. pseudonana* in vivo, instead to the classical method with organic solvents and covalent cross-linking. Via recombinant DNA technology, the authors constructed a fusion gene GFP-GB1 that they introduced via the classical biolistic method into *Thalassiosira* genome. GFP (Green Fluorescence Protein) tag was used to screen the trasformed cells. Then, they loaded the diatoms with chemotherapeutic drugs, demonstrating that diatom biosilica represent a novel, natural and nonotecnologically tailored drug delivery system.

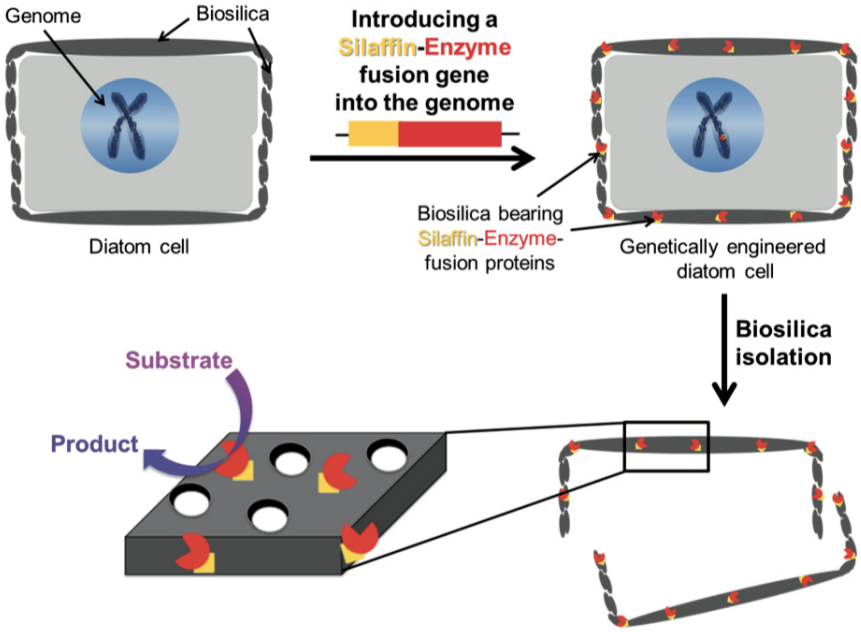

Figure 11. Schematic of the LiDSI method. Reproduced with permission from Ref. [84].

Another approach linking genetic modification and frustule functionalization has been very recently proposed by Wallace and colleagues [125]. It is already well known that there are two main classes of biomolecules involved in diatom biosilicification: phosphorylated proteins and long-chain polyamines. The first type of proteins are polypeptides rich in lysine amino acids and exhibiting post-translational modifications (PTMs) [129]. The authors demonstrated that, through PTMs, it is possible to control the structural features of the silica nonoparticles. In particular, they demonstrated that protelytic cleavage of gene encoding for Silacin-1, Sil1, from *C. fusiformis* releases multiple units. All these units can undergo to different PTMs processes such as phosphorilation and methilation. In particular, the authors proved that the PTMs of one specific peptides, named R5, impact on the silica precipitation process and consequently on shape, porosity, and surface of the frustule. The use of the modified peptides technique will enable the control of silica morphology, allowing to obtain nanostructures with controlled size and with many potential applications in nanotechnology [125].

3.6. Conclusions

Diatoms are able to generate large amounts of nanostructured structures, the frustules, simply by replication. Mechanical, fluid-dynamical, and optical properties of frustules have inspired a profusion of applications including optoelectronics, solar energy harvesting, biofuel extraction, biochemical sensing and biomedicine. The opportunity to modify frustule composition, funcionality and morphology by means of advanced physical and chemical techniques allows the further expansion of its possible technological applications. The possibility to finely tune frustule morphology by genetic engeneering will let to obtain natural, self-replicating nanostructures optimized for a specific task.

Author Contributions: The authors contributed equally to the manuscript. All authors have read and agreed to the published version of the manuscript.

Funding: This research received no external funding.

Conflicts of Interest: The authors declare no conflict of interest.

References

1. Kumari, E.; Görlich, S.; Poulsen, N.; Kröger, N. Genetically Programmed Regioselective Immobilization of Enzymes in Biosilica Microparticles. *Adv. Funct. Mater.* **2020**, *30*, 2000442. [CrossRef]
2. Livage, J. Bioinspired nanostructured materials. *Comptes Rendus Chim.* **2018**, *21*, 969–973. [CrossRef]
3. Otzen, D. The role of proteins in biosilicification. *Scientifica* **2012**, *2012*, 867562. [CrossRef] [PubMed]
4. Perry, C.C.; Keeling-Tucker, T. Biosilicification: the role of the organic matrix in structure control. *JBIC J. Biol. Inorg. Chem.* **2000**, *5*, 537–550. [CrossRef]
5. Hildebrand, M.; Lerch, S.J.; Shrestha, R.P. Understanding diatom cell wall silicification—Moving forward. *Front. Mar. Sci.* **2018**, *5*, 125. [CrossRef]
6. Round, F.E.; Crawford, R.M.; Mann, D.G. *Diatoms: Biology and Morphology of the Genera*; Cambridge University Press: Cambridge, UK, 2007.
7. Nelson, D.M.; Tréguer, P.; Brzezinski, M.A.; Leynaert, A.; Quéguiner, B. Production and dissolution of biogenic silica in the ocean: revised global estimates, comparison with regional data and relationship to biogenic sedimentation. *Glob. Biogeochem. Cycles* **1995**, *9*, 359–372. [CrossRef]
8. Falkowski, P.G.; Raven, J.A. *Aquatic Photosynthesis*; Princeton University Press: Princeton, NJ, USA, 2013.
9. Heintze, C.; Formanek, P.; Pohl, D.; Hauptstein, J.; Rellinghaus, B.; Kröger, N. An intimate view into the silica deposition vesicles of diatoms. *BMC Mater.* **2020**, *2*, 11. [CrossRef]
10. De Tommasi, E.; Gielis, J.; Rogato, A. Diatom frustule morphogenesis and function: A multidisciplinary survey. *Mar. Genom.* **2017**, *35*, 1–18. [CrossRef]
11. Hamm, C.E.; Merkel, R.; Springer, O.; Jurkojc, P.; Maier, C.; Prechtel, K.; Smetacek, V. Architecture and material properties of diatom shells provide effective mechanical protection. *Nature* **2003**, *421*, 841–843. [CrossRef]
12. Hale, M.S.; Mitchell, J.G. Functional morphology of diatom frustule microstructures: hydrodynamic control of Brownian particle diffusion and advection. *Aquat. Microb. Ecol.* **2001**, *24*, 287–295. [CrossRef]
13. Hale, M.S.; Mitchell, J.G. Effects of particle size, flow velocity, and cell surface microtopography on the motion of submicrometer particles over diatoms. *Nano Lett.* **2002**, *2*, 657–663. [CrossRef]
14. Waite, A.; Fisher, A.; Thompson, P.A.; Harrison, P.J. Sinking rate versus cell volume relationships illuminate sinking rate control mechanisms in marine diatoms. *Mar. Ecol. Prog. Ser.* **1997**, *157*, 97–108. [CrossRef]
15. De Tommasi, E. Light manipulation by single cells: the case of diatoms. *J. Spectrosc.* **2016**, *2016*, 2490128. [CrossRef]
16. De Tommasi, E.; De Luca, A.; Lavanga, L.; Dardano, P.; De Stefano, M.; De Stefano, L.; Langella, C.; Rendina, I.; Dholakia, K.; Mazilu, M. Biologically enabled sub-diffractive focusing. *Opt. Express* **2014**, *22*, 27214–27227. [CrossRef] [PubMed]
17. Yang, J.; Zhen, L.; Ren, F.; Campbell, J.; Rorrer, G.L.; Wang, A.X. Ultra-sensitive immunoassay biosensors using hybrid plasmonic-biosilica nanostructured materials. *J. Biophotonics* **2015**, *8*, 659–667. [CrossRef] [PubMed]
18. Lee, S.J.; Huang, C.H.; Shian, S.; Sandhage, K.H. Rapid Hydrolysis of Organophosphorous Esters Induced by Nanostructured, Fluorine-Doped Titania Replicas of Diatom Frustules. *J. Am. Ceram. Soc.* **2007**, *90*, 1632–1636. [CrossRef]
19. Squire, K.; Kong, X.; LeDuff, P.; Rorrer, G.L.; Wang, A.X. Photonic crystal enhanced fluorescence immunoassay on diatom biosilica. *J. Biophotonics* **2018**, *11*, e201800009. [CrossRef]
20. Toster, J.; Iyer, K.S.; Xiang, W.; Rosei, F.; Spiccia, L.; Raston, C.L. Diatom frustules as light traps enhance DSSC efficiency. *Nanoscale* **2013**, *5*, 873–876. [CrossRef]
21. Aw, M.S.; Simovic, S.; Addai-Mensah, J.; Losic, D. Silica microcapsules from diatoms as new carrier for delivery of therapeutics. *Nanomedicine* **2011**, *6*, 1159–1173. [CrossRef]
22. Gordon, R.; Losic, D.; Tiffany, M.A.; Nagy, S.S.; Sterrenburg, F.A. The glass menagerie: diatoms for novel applications in nanotechnology. *Trends Biotechnol.* **2009**, *27*, 116–127. [CrossRef]
23. Friedrichs, L.; Maier, M.; Hamm, C. A new method for exact three-dimensional reconstructions of diatom frustules. *J. Microsc.* **2012**, *248*, 208–217. [CrossRef] [PubMed]
24. Morales, L.V.; Sigman, D.M.; Horn, M.G.; Robinson, R.S. Cleaning methods for the isotopic determination of diatombound nitrogen in non-fossil diatom frustules. *Limnol. Oceanogr. Methods* **2013**, *11*, 101–112. [CrossRef]

25. Romann, J.; Chauton, M.S.; Hanetho, S.M.; Vebner, M.; Heldal, M.; Thaulow, C.; Vadstein, O.; Tranell, G.; Einarsrud, M.A. Diatom frustules as a biomaterial: effects of chemical treatment on organic material removal and mechanical properties in cleaned frustules from two Coscinodiscus species. *J. Porous Mater.* **2016**, *23*, 905–910. [CrossRef]
26. Wang, Y.; Zhang, D.; Cai, J.; Pan, J.; Chen, M.; Li, A.; Jiang, Y. Biosilica structures obtained from Nitzschia, Ditylum, Skeletonema, and Coscinodiscus diatom by a filtration-aided acid cleaning method. *Appl. Microbiol. Biotechnol.* **2012**, *95*, 1165–1178. [CrossRef]
27. Gholami, P.; Khataee, A.; Bhatnagar, A. Environmentally superior cleaning of diatom frustules using sono-Fenton process: Facile fabrication of nanoporous silica with homogeneous morphology and controlled size. *Ultrason. Sonochem.* **2020**, *64*, 105044. [CrossRef]
28. Losic, D.; Short, K.; Mitchell, J.G.; Lal, R.; Voelcker, N.H. AFM nanoindentations of diatom biosilica surfaces. *Langmuir* **2007**, *23*, 5014–5021. [CrossRef]
29. Brzozowska, W.; Sprynskyy, M.; Wojtczak, I.; Dąbek, P.; Witkowski, A.; Buszewski, B. "Outsourcing" Diatoms in Fabrication of Metal-Doped 3D Biosilica. *Materials* **2020**, *13*, 2576. [CrossRef]
30. Jeffryes, C.; Gutu, T.; Jiao, J.; Rorrer, G.L. Two-stage photobioreactor process for the metabolic insertion of nanostructured germanium into the silica microstructure of the diatom Pinnularia sp. *Mater. Sci. Eng. C* **2008**, *28*, 107–118. [CrossRef]
31. De Tommasi, E.; Congestri, R.; Dardano, P.; De Luca, A.C.; Managò, S.; Rea, I.; De Stefano, M. UV-shielding and wavelength conversion by centric diatom nanopatterned frustules. *Sci. Rep.* **2018**, *8*, 1–14. [CrossRef]
32. Qin, T.; Gutu, T.; Jiao, J.; Chang, C.H.; Rorrer, G.L. Photoluminescence of silica nanostructures from bioreactor culture of marine diatom Nitzschia frustulum. *J. Nanosci. Nanotechnol.* **2008**, *8*, 2392–2398. [CrossRef]
33. Jeffryes, C.; Solanki, R.; Rangineni, Y.; Wang, W.; Chang, C.h.; Rorrer, G.L. Electroluminescence and photoluminescence from nanostructured diatom frustules containing metabolically inserted germanium. *Adv. Mater.* **2008**, *20*, 2633–2637. [CrossRef]
34. Gössling, J.W. Biophotonics of Diatoms: Linking Frustule Structure to Photobiology. Ph.D. Thesis, Department of Biology, Faculty of Science, University of Copenhagen, Copenhagen, Denmark, 2017.
35. Townley, H.E.; Woon, K.L.; Payne, F.P.; White-Cooper, H.; Parker, A.R. Modification of the physical and optical properties of the frustule of the diatom Coscinodiscus wailesii by nickel sulfate. *Nanotechnology* **2007**, *18*, 295101. [CrossRef]
36. Jeffryes, C.; Gutu, T.; Jiao, J.; Rorrer, G.L. Metabolic insertion of nanostructured TiO2 into the patterned biosilica of the diatom Pinnularia sp. by a two-stage bioreactor cultivation process. *ACS Nano* **2008**, *2*, 2103–2112. [CrossRef] [PubMed]
37. Jeffryes, C.; Campbell, J.; Li, H.; Jiao, J.; Rorrer, G. The potential of diatom nanobiotechnology for applications in solar cells, batteries, and electroluminescent devices. *Energy Environ. Sci.* **2011**, *4*, 3930–3941. [CrossRef]
38. Gautam, S.; Kashyap, M.; Gupta, S.; Kumar, V.; Schoefs, B.; Gordon, R.; Jeffryes, C.; Joshi, K.B.; Vinayak, V. Metabolic engineering of tio 2 nanoparticles in nitzschia palea to form diatom nanotubes: An ingredient for solar cells to produce electricity and biofuel. *RSC Adv.* **2016**, *6*, 97276–97284. [CrossRef]
39. Bandara, T.; Furlani, M.; Albinsson, I.; Wulff, A.; Mellander, B.E. Diatom frustules enhancing the efficiency of gel polymer electrolyte based dye-sensitized solar cells with multilayer photoelectrodes. *Nanoscale Adv.* **2020**, *2*, 199–209. [CrossRef]
40. Xiao, X.; Zhang, X.; Su, H.; Chen, S.; He, Z.; Zhao, C.; Yang, S. A Visible-NIR Responsive Dye-Sensitized Solar Cell Based on Diatom Frustules and Cosensitization of Photopigments from Diatom and Purple Bacteria. *J. Chem.* **2020**, *2020*, 1710989. [CrossRef]
41. Machill, S.; Köhler, L.; Ueberlein, S.; Hedrich, R.; Kunaschk, M.; Paasch, S.; Schulze, R.; Brunner, E. Analytical studies on the incorporation of aluminium in the cell walls of the marine diatom Stephanopyxis turris. *BioMetals* **2013**, *26*, 141–150. [CrossRef]
42. Zhang, G.; Jiang, W.; Wang, L.; Liao, X.; Liu, P.; Deng, X.; Li, J. Preparation of silicate-based red phosphors with a patterned nanostructure via metabolic insertion of europium in marine diatoms. *Mater. Lett.* **2013**, *110*, 253–255. [CrossRef]
43. Leone, G.; Vona, D.; Presti, M.L.; Urbano, L.; Cicco, S.; Gristina, R.; Palumbo, F.; Ragni, R.; Farinola, G. Ca 2+-in vivo doped biosilica from living Thalassiosira weissflogii diatoms: investigation on Saos-2 biocompatibility. *MRS Adv.* **2017**, *2*, 1047–1058. [CrossRef]

44. Basharina, T.N.; Danilovtseva, E.N.; Zelinskiy, S.N.; Klimenkov, I.V.; Likhoshway, Y.V.; Annenkov, V.V. The effect of titanium, zirconium and tin on the growth of diatom Synedra acus and morphology of its silica valves. *Silicon* **2012**, *4*, 239–249. [CrossRef]
45. Gannavarapu, K.P.; Ganesh, V.; Thakkar, M.; Mitra, S.; Dandamudi, R.B. Nanostructured Diatom-ZrO2 composite as a selective and highly sensitive enzyme free electrochemical sensor for detection of methyl parathion. *Sens. Actuators B Chem.* **2019**, *288*, 611–617. [CrossRef] [PubMed]
46. Kucki, M. Biological Photonic Crystals: Diatoms Dye Functionalization of Biological Silica Nanostructures. Ph.D. Thesis, University of Kassel, Kassel, Germany, 2009.
47. Kucki, M.; Fuhrmann-Lieker, T. Staining diatoms with rhodamine dyes: control of emission colour in photonic biocomposites. *J. R. Soc. Interface* **2012**, *9*, 727–733. [CrossRef] [PubMed]
48. Megens, M.; Wijnhoven, J.E.; Lagendijk, A.; Vos, W.L. Fluorescence lifetimes and linewidths of dye in photonic crystals. *Phys. Rev. A* **1999**, *59*, 4727. [CrossRef]
49. Yoshie, T.; Shchekin, O.; Chen, H.; Deppe, D.; Scherer, A. Quantum dot photonic crystal lasers. *Electron. Lett.* **2002**, *38*, 967–968. [CrossRef]
50. Ragni, R.; Scotognella, F.; Vona, D.; Moretti, L.; Altamura, E.; Ceccone, G.; Mehn, D.; Cicco, S.R.; Palumbo, F.; Lanzani, G.; et al. Hybrid photonic nanostructures by in vivo incorporation of an organic fluorophore into diatom algae. *Adv. Funct. Mater.* **2018**, *28*, 1706214. [CrossRef]
51. Fuhrmann, T.; Landwehr, S.; El Rharbi-Kucki, M.; Sumper, M. Diatoms as living photonic crystals. *Appl. Phys. B* **2004**, *78*, 257–260. [CrossRef]
52. Yamanaka, S.; Yano, R.; Usami, H.; Hayashida, N.; Ohguchi, M.; Takeda, H.; Yoshino, K. Optical properties of diatom silica frustule with special reference to blue light. *J. Appl. Phys.* **2008**, *103*, 074701. [CrossRef]
53. De Stefano, L.; Maddalena, P.; Moretti, L.; Rea, I.; Rendina, I.; De Tommasi, E.; Mocella, V.; De Stefano, M. Nano-biosilica from marine diatoms: A brand new material for photonic applications. *Superlattices Microstruct.* **2009**, *46*, 84–89. [CrossRef]
54. Kieu, K.; Li, C.; Fang, Y.; Cohoon, G.; Herrera, O.; Hildebrand, M.; Sandhage, K.; Norwood, R.A. Structure-based optical filtering by the silica microshell of the centric marine diatom Coscinodiscus wailesii. *Opt. Express* **2014**, *22*, 15992–15999. [CrossRef]
55. Mcheik, A.; Cassaignon, S.; Livage, J.; Gibaud, A.; Berthier, S.; Lopez, P.J. Optical properties of nanostructured silica structures from marine organisms. *Front. Mar. Sci.* **2018**, *5*, 123. [CrossRef]
56. Goessling, J.W.; Su, Y.; Cartaxana, P.; Maibohm, C.; Rickelt, L.F.; Trampe, E.C.; Walby, S.L.; Wangpraseurt, D.; Wu, X.; Ellegaard, M.; et al. Structure-based optics of centric diatom frustules: modulation of the in vivo light field for efficient diatom photosynthesis. *New Phytol.* **2018**, *219*, 122–134. [CrossRef] [PubMed]
57. Goessling, J.W.; Paul, V.; Ashworth, M.; Manning, S.R.; Lopez-Garcia, M.; Gonzalez, A.A.S. Biosilica slab photonic crystals as an alternative to cleanroom fabrication. *Faraday Discuss.* **2020**, *223*. [CrossRef]
58. Goessling, J.W.; Wardley, W.P.; Lopez-Garcia, M. Highly Reproducible, Bio-Based Slab Photonic Crystals Grown by Diatoms. *Adv. Sci.* **2020**, *7*, 1903726. [CrossRef] [PubMed]
59. Sakoda, K. *Optical Properties of Photonic Crystals*; Springer Science & Business Media: Berlin/Heidelberg, Germany, 2004; Volume 80.
60. Joannopoulos, J.D.; Johnson, S.G.; Winn, J.N.; Meade, R.D. *Molding the Flow of Light*; Princeton University Press: Princeton, NJ, USA, 2008.
61. Maier, S.A. *Plasmonics: Fundamentals and Applications*; Springer Science & Business Media: Berlin/Heidelberg, Germany, 2007.
62. Le Ru, E.; Etchegoin, P. *Principles of Surface-Enhanced Raman Spectroscopy: Furthermore, Related Plasmonic Effects*; Elsevier: Amsterdam, The Netherlands, 2008.
63. Lee, P.; Meisel, D. Adsorption and surface-enhanced Raman of dyes on silver and gold sols. *J. Phys. Chem.* **1982**, *86*, 3391–3395. [CrossRef]
64. Liz-Marzán, L.M.; Giersig, M.; Mulvaney, P. Synthesis of nanosized gold-silica core-shell particles. *Langmuir* **1996**, *12*, 4329–4335. [CrossRef]
65. Tao, A.; Kim, F.; Hess, C.; Goldberger, J.; He, R.; Sun, Y.; Xia, Y.; Yang, P. Langmuir-Blodgett silver nanowire monolayers for molecular sensing using surface-enhanced Raman spectroscopy. *Nano Lett.* **2003**, *3*, 1229–1233. [CrossRef]
66. Sun, Y.; Xia, Y. Shape-controlled synthesis of gold and silver nanoparticles. *Science* **2002**, *298*, 2176–2179. [CrossRef]

67. McLellan, J.M.; Li, Z.Y.; Siekkinen, A.R.; Xia, Y. The SERS activity of a supported Ag nanocube strongly depends on its orientation relative to laser polarization. *Nano Lett.* **2007**, *7*, 1013–1017. [CrossRef]
68. Hrelescu, C.; Sau, T.K.; Rogach, A.L.; Jäckel, F.; Feldmann, J. Single gold nanostars enhance Raman scattering. *Appl. Phys. Lett.* **2009**, *94*, 153113. [CrossRef]
69. Matteini, P.; Cottat, M.; Tavanti, F.; Panfilova, E.; Scuderi, M.; Nicotra, G.; Menziani, M.C.; Khlebtsov, N.; de Angelis, M.; Pini, R. Site-selective surface-enhanced Raman detection of proteins. *ACS Nano* **2017**, *11*, 918–926. [CrossRef] [PubMed]
70. Muehlschlegel, P.; Eisler, H.J.; Martin, O.J.; Hecht, B.; Pohl, D. Resonant optical antennas. *Science* **2005**, *308*, 1607–1609. [CrossRef] [PubMed]
71. Crozier, K.B.; Zhu, W.; Wang, D.; Lin, S.; Best, M.D.; Camden, J.P. Plasmonics for surface enhanced raman scattering: Nanoantennas for single molecules. *IEEE J. Sel. Top. Quantum Electron.* **2013**, *20*, 152–162. [CrossRef]
72. Jiao, Y.; Ryckman, J.D.; Ciesielski, P.N.; Escobar, C.A.; Jennings, G.K.; Weiss, S.M. Patterned nanoporous gold as an effective SERS template. *Nanotechnology* **2011**, *22*, 295302. [CrossRef]
73. Kim, S.m.; Zhang, W.; Cunningham, B.T. Coupling discrete metal nanoparticles to photonic crystal surface resonant modes and application to Raman spectroscopy. *Opt. Express* **2010**, *18*, 4300–4309. [CrossRef]
74. Ricciardi, A.; Consales, M.; Quero, G.; Crescitelli, A.; Esposito, E.; Cusano, A. Versatile optical fiber nanoprobes: from plasmonic biosensors to polarization-sensitive devices. *ACS Photonics* **2014**, *1*, 69–78. [CrossRef]
75. De Luca, A.C.; Reader-Harris, P.; Mazilu, M.; Mariggio, S.; Corda, D.; Di Falco, A. Reproducible surface-enhanced Raman quantification of biomarkers in multicomponent mixtures. *ACS Nano* **2014**, *8*, 2575–2583. [CrossRef]
76. De Angelis, F.; Malerba, M.; Patrini, M.; Miele, E.; Das, G.; Toma, A.; Zaccaria, R.P.; Di Fabrizio, E. 3D hollow nanostructures as building blocks for multifunctional plasmonics. *Nano Lett.* **2013**, *13*, 3553–3558. [CrossRef]
77. Payne, E.K.; Rosi, N.L.; Xue, C.; Mirkin, C.A. Sacrificial biological templates for the formation of nanostructured metallic microshells. *Angew. Chem.* **2005**, *117*, 5192–5195. [CrossRef]
78. Ren, F.; Campbell, J.; Rorrer, G.L.; Wang, A.X. Surface-enhanced Raman spectroscopy sensors from nanobiosilica with self-assembled plasmonic nanoparticles. *IEEE J. Sel. Top. Quantum Electron.* **2014**, *20*, 127–132.
79. Kamińska, A.; Sprynskyy, M.; Winkler, K.; Szymborski, T. Ultrasensitive SERS immunoassay based on diatom biosilica for detection of interleukins in blood plasma. *Anal. Bioanal. Chem.* **2017**, *409*, 6337–6347. [CrossRef] [PubMed]
80. Managò, S.; Zito, G.; Rogato, A.; Casalino, M.; Esposito, E.; De Luca, A.C.; De Tommasi, E. Bioderived three-dimensional hierarchical nanostructures as efficient surface-enhanced raman scattering substrates for cell membrane probing. *ACS Appl. Mater. Interfaces* **2018**, *10*, 12406–12416. [CrossRef] [PubMed]
81. Sivashanmugan, K.; Squire, K.; Kraai, J.A.; Tan, A.; Zhao, Y.; Rorrer, G.L.; Wang, A.X. Biological Photonic Crystal-Enhanced Plasmonic Mesocapsules: Approaching Single-Molecule Optofluidic-SERS Sensing. *Adv. Opt. Mater.* **2019**, *7*, 1900415. [CrossRef] [PubMed]
82. Fang, Y.; Chen, V.W.; Cai, Y.; Berrigan, J.D.; Marder, S.R.; Perry, J.W.; Sandhage, K.H. Biologically Enabled Syntheses of Freestanding Metallic Structures Possessing Subwavelength Pore Arrays for Extraordinary (Surface Plasmon-Mediated) Infrared Transmission. *Adv. Funct. Mater.* **2012**, *22*, 2550–2559. [CrossRef]
83. Pacifici, D.; Lezec, H.J.; Sweatlock, L.A.; Walters, R.J.; Atwater, H.A. Universal optical transmission features in periodic and quasiperiodic hole arrays. *Opt. Express* **2008**, *16*, 9222–9238. [CrossRef]
84. Kröger, N.; Dubey, N.; Kumari, E. Immobilization of Proteins on Diatom Biosilica. In *Diatom Nanotechnology*; Royal Society of Chemistry: London, UK, 2017; pp. 126–149.
85. Dill, K.A.; Ghosh, K.; Schmit, J.D. Physical limits of cells and proteomes. *Proc. Natl. Acad. Sci. USA* **2011**, *108*, 17876–17882. [CrossRef]
86. Townley, H.E.; Parker, A.R.; White-Cooper, H. Exploitation of diatom frustules for nanotechnology: Tethering active biomolecules. *Adv. Funct. Mater.* **2008**, *18*, 369–374. [CrossRef]
87. De Stefano, L.; Lamberti, A.; Rotiroti, L.; De Stefano, M. Interfacing the nanostructured biosilica microshells of the marine diatom Coscinodiscus wailesii with biological matter. *Acta Biomater.* **2008**, *4*, 126–130. [CrossRef]

88. De Tommasi, E.; Rea, I.; Rendina, I.; Rotiroti, L.; De Stefano, L. Protein conformational changes revealed by optical spectroscopic reflectometry in porous silicon multilayers. *J. Phys. Condens. Matter* **2008**, *21*, 035115. [CrossRef]
89. De Tommasi, E.; De Stefano, L.; Rea, I.; Di Sarno, V.; Rotiroti, L.; Arcari, P.; Lamberti, A.; Sanges, C.; Rendina, I. Porous silicon based resonant mirrors for biochemical sensing. *Sensors* **2008**, *8*, 6549–6556. [CrossRef]
90. Hilkens, J.; Ligtenberg, M.J.; Vos, H.L.; Litvinov, S.V. Cell membrane-associated mucins and their adhesion-modulating property. *Trends Biochem. Sci.* **1992**, *17*, 359–363. [CrossRef]
91. Bayramoglu, G.; Akbulut, A.; Arica, M.Y. Immobilization of tyrosinase on modified diatom biosilica: Enzymatic removal of phenolic compounds from aqueous solution. *J. Hazard. Mater.* **2013**, *244*, 528–536. [CrossRef] [PubMed]
92. Bayramoglu, G.; Akbulut, A.; Ozalp, V.C.; Arica, M.Y. Immobilized lipase on micro-porous biosilica for enzymatic transesterification of algal oil. *Chem. Eng. Res. Des.* **2015**, *95*, 12–21. [CrossRef]
93. De Stefano, L.; Rotiroti, L.; De Stefano, M.; Lamberti, A.; Lettieri, S.; Setaro, A.; Maddalena, P. Marine diatoms as optical biosensors. *Biosens. Bioelectron.* **2009**, *24*, 1580–1584. [CrossRef]
94. Losic, D.; Mitchell, J.G.; Voelcker, N.H. Diatomaceous lessons in nanotechnology and advanced materials. *Adv. Mater.* **2009**, *21*, 2947–2958. [CrossRef]
95. Ragni, R.; Cicco, S.R.; Vona, D.; Farinola, G.M. Multiple routes to smart nanostructured materials from diatom microalgae: A chemical perspective. *Adv. Mater.* **2018**, *30*, 1704289. [CrossRef]
96. Panwar, V.; Dutta, T. Diatom biogenic silica as a felicitous platform for biochemical engineering: Expanding frontiers. *ACS Appl. Bio Mater.* **2019**, *2*, 2295–2316. [CrossRef]
97. De Stefano, L.; Rendina, I.; De Stefano, M.; Bismuto, A.; Maddalena, P. Marine diatoms as optical chemical sensors. *Appl. Phys. Lett.* **2005**, *87*, 233902. [CrossRef]
98. Setaro, A.; Lettieri, S.; Maddalena, P.; De Stefano, L. Highly sensitive optochemical gas detection by luminescent marine diatoms. *Appl. Phys. Lett.* **2007**, *91*, 051921. [CrossRef]
99. Lettieri, S.; Setaro, A.; De Stefano, L.; De Stefano, M.; Maddalena, P. The gas-detection properties of light-emitting diatoms. *Adv. Funct. Mater.* **2008**, *18*, 1257–1264. [CrossRef]
100. Gale, D.K.; Gutu, T.; Jiao, J.; Chang, C.H.; Rorrer, G.L. Photoluminescence detection of biomolecules by antibody-functionalized diatom biosilica. *Adv. Funct. Mater.* **2009**, *19*, 926–933. [CrossRef]
101. Losic, D.; Mitchell, J.G.; Lal, R.; Voelcker, N.H. Rapid fabrication of micro-and nanoscale patterns by replica molding from diatom biosilica. *Adv. Funct. Mater.* **2007**, *17*, 2439–2446. [CrossRef]
102. Bao, Z.; Weatherspoon, M.R.; Shian, S.; Cai, Y.; Graham, P.D.; Allan, S.M.; Ahmad, G.; Dickerson, M.B.; Church, B.C.; Kang, Z.; et al. Chemical reduction of three-dimensional silica micro-assemblies into microporous silicon replicas. *Nature* **2007**, *446*, 172–175. [CrossRef] [PubMed]
103. Pan, Z.; Lerch, S.J.; Xu, L.; Li, X.; Chuang, Y.J.; Howe, J.Y.; Mahurin, S.M.; Dai, S.; Hildebrand, M. Electronically transparent graphene replicas of diatoms: A new technique for the investigation of frustule morphology. *Sci. Rep.* **2014**, *4*, 6117. [CrossRef] [PubMed]
104. Li, K.; Liu, X.; Zheng, T.; Jiang, D.; Zhou, Z.; Liu, C.; Zhang, X.; Zhang, Y.; Losic, D. Tuning MnO2 to FeOOH replicas with bio-template 3D morphology as electrodes for high performance asymmetric supercapacitors. *Chem. Eng. J.* **2019**, *370*, 136–147. [CrossRef]
105. Xu, M.; Gratson, G.M.; Duoss, E.B.; Shepherd, R.F.; Lewis, J.A. Biomimetic silicification of 3D polyamine-rich scaffolds assembled by direct ink writing. *Soft Matter* **2006**, *2*, 205–209. [CrossRef]
106. Gratson, G.M.; Xu, M.; Lewis, J.A. Direct writing of three-dimensional webs. *Nature* **2004**, *428*, 386. [CrossRef]
107. Xie, P.; Chen, Z.; Xu, J.; Xie, D.; Wang, X.; Cui, S.; Zhou, H.; Zhang, D.; Fan, T. Artificial ceramic diatoms with multiscale photonic architectures via nanoimprint lithography for CO2 photoreduction. *J. Am. Ceram. Soc.* **2019**, *102*, 4678–4687. [CrossRef]
108. Kröger, N.; Bergsdorf, C.; Sumper, M. Frustulins: domain conservation in a protein family associated with diatom cell walls. *Eur. J. Biochem.* **1996**, *239*, 259–264. [CrossRef]
109. Heintze, C.; Formanek, P.; Pohl, D.; Hauptstein, J.; Rellinghaus, B.; Kröger, N. A New View into the Silica Deposition Vesicles of Diatoms. 2020. Available online: https://assets.researchsquare.com/files/rs-22354/v3/a9518908-f148-4d7c-9440-5424fc0fe15e.pdf (accessed on 15 June 2020).
110. Kroth, P. Molecular biology and the biotechnological potential of diatoms. In *Transgenic Microalgae As Green Cell Factories*; Springer: Berlin/Heidelberg, Germany, 2007; pp. 23–33.

111. Zaslavskaia, L.A.; Lippmeier, J.C.; Kroth, P.G.; Grossman, A.R.; Apt, K.E. Transformation of the diatom Phaeodactylum tricornutum (Bacillariophyceae) with a variety of selectable marker and reporter genes. *J. Phycol.* **2000**, *36*, 379–386. [CrossRef]
112. Coesel, S.; Mangogna, M.; Ishikawa, T.; Heijde, M.; Rogato, A.; Finazzi, G.; Todo, T.; Bowler, C.; Falciatore, A. Diatom PtCPF1 is a new cryptochrome/photolyase family member with DNA repair and transcription regulation activity. *EMBO Rep.* **2009**, *10*, 655–661. [CrossRef] [PubMed]
113. De Riso, V.; Raniello, R.; Maumus, F.; Rogato, A.; Bowler, C.; Falciatore, A. Gene silencing in the marine diatom Phaeodactylum tricornutum. *Nucleic Acids Res.* **2009**, *37*, e96. [CrossRef] [PubMed]
114. Weyman, P.D.; Beeri, K.; Lefebvre, S.C.; Rivera, J.; McCarthy, J.K.; Heuberger, A.L.; Peers, G.; Allen, A.E.; Dupont, C.L. Inactivation of P haeodactylum tricornutum urease gene using transcription activator-like effector nuclease-based targeted mutagenesis. *Plant Biotechnol. J.* **2015**, *13*, 460–470. [CrossRef]
115. Nymark, M.; Sharma, A.K.; Sparstad, T.; Bones, A.M.; Winge, P. A CRISPR/Cas9 system adapted for gene editing in marine algae. *Sci. Rep.* **2016**, *6*, 24951. [CrossRef] [PubMed]
116. Huang, W.; Daboussi, F. Genetic and metabolic engineering in diatoms. *Philos. Trans. R. Soc. B Biol. Sci.* **2017**, *372*, 20160411. [CrossRef]
117. Kroth, P.G.; Bones, A.M.; Daboussi, F.; Ferrante, M.I.; Jaubert, M.; Kolot, M.; Nymark, M.; Bártulos, C.R.; Ritter, A.; Russo, M.T.; et al. Genome editing in diatoms: achievements and goals. *Plant Cell Rep.* **2018**, *37*, 1401–1408. [CrossRef]
118. Görlich, S.; Pawolski, D.; Zlotnikov, I.; Kröger, N. Control of biosilica morphology and mechanical performance by the conserved diatom gene Silicanin-1. *Commun. Biol.* **2019**, *2*, 1–8. [CrossRef]
119. Rogato, A.; Del Prete, S.; Nocentini, A.; Carginale, V.; Supuran, C.T.; Capasso, C. Phaeodactylum tricornutum as a model organism for testing the membrane penetrability of sulphonamide carbonic anhydrase inhibitors. *J. Enzym. Inhib. Med. Chem.* **2019**, *34*, 510–518. [CrossRef]
120. Tesson, B.; Lerch, S.J.; Hildebrand, M. Characterization of a new protein family associated with the silica deposition vesicle membrane enables genetic manipulation of diatom silica. *Sci. Rep.* **2017**, *7*, 1–13. [CrossRef]
121. Shrestha, R.P.; Hildebrand, M. Evidence for a regulatory role of diatom silicon transporters in cellular silicon responses. *Eukaryot. Cell* **2015**, *14*, 29–40. [CrossRef]
122. Knight, M.J.; Senior, L.; Nancolas, B.; Ratcliffe, S.; Curnow, P. Direct evidence of the molecular basis for biological silicon transport. *Nat. Commun.* **2016**, *7*, 1–11. [CrossRef] [PubMed]
123. Delalat, B.; Sheppard, V.C.; Ghaemi, S.R.; Rao, S.; Prestidge, C.A.; McPhee, G.; Rogers, M.L.; Donoghue, J.F.; Pillay, V.; Johns, T.G.; et al. Targeted drug delivery using genetically engineered diatom biosilica. *Nat. Commun.* **2015**, *6*, 1–11. [CrossRef] [PubMed]
124. Kotzsch, A.; Gröger, P.; Pawolski, D.; Bomans, P.H.; Sommerdijk, N.A.; Schlierf, M.; Kröger, N. Silicanin-1 is a conserved diatom membrane protein involved in silica biomineralization. *BMC Biol.* **2017**, *15*, 65. [CrossRef] [PubMed]
125. Wallace, A.K.; Chanut, N.; Voigt, C.A. Silica Nanostructures Produced Using Diatom Peptides with Designed Post-Translational Modifications. *Adv. Funct. Mater.* **2020**, *30*, 2000849. [CrossRef]
126. Shrestha, R.P.; Tesson, B.; Norden-Krichmar, T.; Federowicz, S.; Hildebrand, M.; Allen, A.E. Whole transcriptome analysis of the silicon response of the diatom Thalassiosira pseudonana. *BMC Genom.* **2012**, *13*, 499. [CrossRef]
127. Poulsen, N.; Berne, C.; Spain, J.; Kroeger, N. Silica immobilization of an enzyme through genetic engineering of the diatom Thalassiosira pseudonana. *Angew. Chem. Int. Ed.* **2007**, *46*, 1843–1846. [CrossRef]
128. Sheppard, V.; Scheffel, A.; Poulsen, N.; Kröger, N. Live diatom silica immobilization of multimeric and redox-active enzymes. *Appl. Environ. Microbiol.* **2012**, *78*, 211–218. [CrossRef]
129. Fernandes, F.M.; Coradin, T.; Aimé, C. Self-assembly in biosilicification and biotemplated silica materials. *Nanomaterials* **2014**, *4*, 792–812. [CrossRef]